Demonstration of Quantum Entanglement between a Single Electron Spin Confined to an InAs Quantum Dot and a Photon

J. R. Schaibley, A. P. Burgers, G. A. McCracken, L.-M. Duan, P. R. Berman, D. G. Steel, A. S. Bracker, D. Gammon, and L. J. Sham

Phys. Rev. Lett. **110**, 167401 — Published 16 April 2013

DOI: 10.1103/PhysRevLett.110.167401

Demonstration of quantum entanglement between a single electron spin confined to an InAs quantum dot and a photon

J. R. Schaibley, A. P. Burgers, G. A. McCracken, L-M Duan, P. R. Berman, and D. G. Steel*

The H. M. Randall Laboratory of Physics,

The University of Michigan, Ann Arbor, Michigan 48109-1040, USA

A. S. Bracker and D. Gammon

The Naval Research Laboratory, Washington D.C. 20375, USA

L. J. Sham

Department of Physics, The University of California,

San Diego, La Jolla, California, 92093-0319, USA

(Dated: March 4, 2013)

Abstract

The electron spin state of a singly charged semiconductor quantum dot has been shown to form a suitable single qubit for quantum computing architectures with fast gate times. A key challenge in realizing a useful quantum dot quantum computing architecture lies in demonstrating the ability to scale the system to many qubits. In this letter, we report an all optical experimental demonstration of quantum entanglement between a single electron spin confined to single charged semiconductor quantum dot and the polarization state of a photon spontaneously emitted from the quantum dot's excited state. We obtain a lower bound on the fidelity of entanglement of 0.59 ± 0.04, which is 84% of the maximum achievable given the timing resolution of available single photon detectors. In future applications, such as measurement based spin-spin entanglement which does not require sub-nanosecond timing resolution, we estimate that this system would enable near ideal performance. The inferred (usable) entanglement generation rate is 3×10^3 s^{-1}. This spin-photon entanglement is the first step to a scalable quantum dot quantum computing architecture relying on photon (flying) qubits to mediate entanglement between distant nodes of a quantum dot network.

A single electron spin confined to a charged semiconductor quantum dot (QD) can effectively serve as a single quantum storage device with fast information processing for quantum computing architectures [1–3]. QD architectures are excellent candidates for scalable quantum information applications since they are compatible with existing semiconductor processing infrastructure. In addition, site-controlled QD growth has been demonstrated [4, 5], and single QDs have been integrated with photonic crystal cavities [6, 7], offering significant advantages of optically driven QD spins over other modern quantum information systems. In order to construct a scalable architecture, quantum information must be coherently transferrable between electron spin qubits in separate nodes. The photons emitted from an excited, negatively charged QD (called a trion: a multi-particle state comprised of two electrons and one hole) provide an attractive messenger to carry this information. Recently, optical initialization, rotation and readout of a single electron spin qubit in a single QD were accomplished, demonstrating the QD spin's usefulness as a single qubit [8–11]. Scaling the architecture to arbitrary size requires the ability to entangle the spin qubits of spatially distinct QDs, recently demonstrated by using the tunneling interaction between spatially adjacent QDs [12]. One scaling approach that does not require local interactions instead uses photon qubits to entangle the QDs [13–16]. If the photons emitted from two QDs are indistinguishable, coincidence measurements can be performed on the emitted photons to probabilistically entangle the source QDs [13, 14, 17, 18]. The first step in protocols of this nature is establishing the entanglement between a single emitted photon and a single QD spin.

In this letter, we report entanglement between a single electron spin state confined to a single semiconductor QD and the polarization state of a photon that has been emitted spontaneously from the QD's excited state [19]. The entanglement is verified by performing projective measurements on the entangled photon's polarization state and time correlating this detection with the resulting electron spin state of the QD in two bases. The protocol follows established techniques in quantum information systems using single atoms and nitrogen vacancy centers in diamond [20–23]. This demonstration of entanglement represents a hybrid entanglement between an engineered quantum state and a traveling qubit and is integral to future applications using QDs in quantum information and scalable quantum computing applications. The validity of the approach used here and in other recent experiments [22, 23] has recently been justified theoretically. [24].

The energy level structure of a single charged QD in the presence of an externally applied magnetic field (Voigt geometry) is shown in Fig. 1(a) with the corresponding optical selection rules [9]. In the experiment, the QD is initialized to a pure state via optical pumping, then excited to the $|T_x-\rangle$ trion state with a laser pulse, where it then decays to the two ground states with equal probability [9]. When the $|T_x-\rangle$ state decays, the horizontal (vertical) (H,V) polarization state of the emitted photon, collected along the z axis, is correlated with the final state ($|x+\rangle$, $|x-\rangle$) of the QD. Here, the electron ground state frequency splitting ($\Delta_e = 2\pi \times 7.35$ GHz) is larger than the spontaneous emission rate (10^9 s^{-1}), so a fast detector with timing resolution (τ_r) of 48 ps FWHM is used to destroy the which-path information from the frequency mismatch of the two decay channels [21–26]. The resulting state vector ($|\Psi\rangle$) of the system is,

$$|\Psi\rangle = \frac{|H\rangle\,|x+\rangle - i\,|V\rangle\,|x-\rangle}{\sqrt{2}}, \tag{1}$$

clearly reflecting the entanglement [26].

The state of the photon is measured with a single photon avalanche photodiode (SPAPD) after polarization analysis. The measurement of the photon's polarization is correlated uniquely with a particular final state in the QD. A narrow bandwidth laser pulse reads out the resulting electron spin state by selectively scattering from only one of the ground states, mapping the QD spin state into a readout photon which is detected by another SPAPD. The photon and spin measurements are analyzed based on their time correlated nature to reconstruct the state of the spin-photon system. First, we confirm that the detection of a H (V) polarized photon is correlated with the $|x+\rangle(|x-\rangle)$ state of the QD. We then verify that the state is entangled by rotating both measurement bases by $\pi/2$ about the y axis and showing that the measured state of the spin in the z basis ($|z\mp\rangle = \frac{|x+\rangle \pm |x-\rangle}{\sqrt{2}}$) remains correlated with the detection of a circularly polarized photon ($|\sigma\pm\rangle = \frac{|H\rangle \pm i|V\rangle}{\sqrt{2}}$). This is possible due to long coherence time of the QD spin state [27–29].

The system investigated is a single negatively charged InAs QD embedded in a GaAs Schottky diode heterostructure grown via molecular beam epitaxy. The characterization of QDs is discussed in detail in earlier work [9, 30]. Optical studies are performed at ≈ 7 K with a combination of pulses from CW lasers produced by $LiNbO_3$ electro-optic modulators which are synchronized with a 76 MHz mode-locked Ti:Sapphire laser. A 4 ns resonant laser pulse

initializes to either the $|x+\rangle$ or $|x-\rangle$ state of the QD, and a resonant 250 ps ($\Theta_{trion} = \pi$ area) pulse selectively excites this state to $|T_x-\rangle$. The resulting spin state following spontaneous emission is then measured by a resonant state selective readout pulse (either 4 ns or 250 ps). For the rotated ($|z\mp\rangle$,$|\sigma\pm\rangle$) basis measurements, a ≈ 2 ps ($\Theta_{spin} = \pi/2$ area) Raman pulse, red detuned by approximately 1 meV, is used to rotate the z basis state into an x basis state prior to readout by the 4 ns measurement pulse[10, 11]. The pulse widths and magnetic field are chosen to simultaneously allow for frequency selective state excitation, while at the same time keeping the ground state splitting small compared to the bandwidth of our detector. The entangled and readout photons are projected by a polarization analyzer and quarter-wave plate which is used either to convert back to linear polarization or to correct for birefringence in the cryostat's windows. The QD emission is then coupled into a single mode fiber, split with a 50-50 fiber splitter and sent to two SPAPDs in a HBT-type setup [31]. The photon arrival times are time tagged relative to the excitation pulses using a picosecond event timer. For the z basis measurement, a fast timing SPAPD is used to measure the entangled photon's arrival time (timing jitter 48 ps FWHM) that sets the maximum observable spin precession rate (Zeeman splitting). For this QD, that splitting corresponds to a magnetic field of 1.1 T. For each photon projection axis (H,V,$\sigma+$,$\sigma-$), the excitation and rotation lasers were polarized orthogonally to the measurement axis. The QD emission is separated from the excitation lasers by a combination of polarization and spatial filtering. For the rotated ($|z\mp\rangle$, $\sigma\pm$) basis measurements, an air spaced etalon is used to further attenuate the detuned rotation pulse by 30 dB. The rejection ratio of the narrow bandwidth pulses exceeds 70 dB. The probability of false correlations contributing to our signal due to resonant excitation leak through is less than 0.02 for the x basis measurements and less than 0.05 for the z basis measurements. Due to the time correlated nature of the measurements, false correlations from detector dark counts are negligible. The setup's single channel detection efficiency (DE) is $\approx 4 \times 10^{-5}$; the detection efficiency of the fast timing resolution SPAPD required for the z basis measurement is $\approx 4 \times 10^{-6}$.

The experimental pulse sequences are shown in Fig. 2. Six independent measurements are performed to obtain the conditional probabilities shown in Fig. 3. For the H and V measurements, four separate measurements are performed, one for each of the x basis conditional probabilities (Fig. 3(a)). For the $\sigma\pm$ measurements, two separate measurements are performed, each of which simultaneously measures two z basis conditional probabilities

(Fig. 3(b)). In the first measurement, the correlation between a H emitted photon and the $|x+\rangle$ state is established using a two pulse sequence where both pulses are linearly polarized with the vertical (horizontal) transitions (Fig. 2(a)). The QD is initialized to $|x-\rangle$ with a 4 ns ($\Omega_{CW}/2\pi \approx 1$ GHz, where Ω_{CW} is the Rabi frequency) pulse tuned to the V_1 transition. Then a 250 ps pulse (π area), tuned to the V_4 transition, excites the system to $|T_x-\rangle$, followed by spontaneous emission. We then correlate the final state of the QD with the polarization of the emitted photon. The next 4 ns initialization pulse also serves as a readout pulse for the state of the QD. It scatters a photon only if the QD is in the $|x+\rangle$ state. In the event that no photon is collected after the 250 ps pulse, the probability of detecting a readout photon is half as likely, since we have no information on the final state of the QD. In the second measurement, we then perform a negative correlation measurement between H and $|x-\rangle$ by inserting an additional 250 ps (probe) pulse between the existing 250 ps (excitation) pulse and 4 ns pulse (which now serves only to re-initialize). Here, upon detection of a H polarized photon following the first 250 ps pulse, the spin is projected to $|x+\rangle$, so the second 250 ps probe pulse should not scatter any photons off the $|x-\rangle$ state (Fig. 2(b)). This pair of experiments is then repeated with initialization to $|x+\rangle$ using a 4 ns pulse tuned to the H_3 transition and a 250 ps pulse tuned to the H_2 transition. In analogy with the first two measurements, we then establish the correlation between a V emitted photon and $|x-\rangle$ or a negative correlation with $|x+\rangle$. We normalize the conditional probabilities by comparing the number of correlations between the entangled photons and those from the 4 ns or 250 ps readout pulse to the number of correlations between an entangled photon with a readout photon from temporally distant runs of the experiment (which corresponds to a probability of 0.5 for a π excitation pulse).

An example of the time integrated emission from a positive correlation measurement is shown in Fig. 1(b). We measure the probability of recording coincident photons on each of the two SPAPDs during the same pulse and use this to correct the raw data. The corrected data are normalized requiring the sum of each pair to equal one [32]. The corrected conditional probabilities calculated, shown in Fig. 3(a), are: $P(x-|V) = 0.84 \pm 0.04$, $P(x+|V) = 0.16 \pm 0.01$, $P(x+|H) = 0.94 \pm 0.05$, and $P(x-|H) = 0.06 \pm 0.01$. The uncorrected values are: $P(x-|V) = 0.68 \pm 0.02$, $P(x+|V) = 0.25 \pm 0.02$, $P(x+|H) = 0.91 \pm 0.03$, and $P(x-|H) = 0.12 \pm 0.04$. We note that the primary source of error is off-resonant coupling of the laser pulses to the other trion state. This coupling is more

pronounced in the V configuration, where the lasers are driving the H transitions which are the closest in energy, and is manifested in the lower fidelity of the V measurement as well as the sum of the uncorrected conditional probabilities differing further from one. This error is partially corrected by the subtraction method used to obtain the corrected values, but remains detrimental to the fidelity due to imperfect state initialization [32]. The unintended excitation can in principle be removed by pulse shaping [33].

In our final measurements, carried out using the z basis (i.e., the rotated basis), the correlation is time dependent allowing for simultaneous measurement of two conditional probabilities. The 1.1 T magnetic field keeps the ground state precession period longer than the timing resolution of the fast timing resolution SPAPD while splitting the excited states sufficiently to allow frequency selective excitation since the circular polarized laser pulses can couple to either transition. This will lower the fidelity of entanglement because of the reduced quality of initialization into a pure state. For both measurements, the QD is initialized to $|x-\rangle$ with a 4 ns pulse tuned to the V_1 transition and then excited to the $|T_x-\rangle$ state with a 250 ps pulse resonant on the V_4 transition. The excited QD decays to both lower spin states. The photon state is measured along $\sigma\pm$, which projects the QD spin to a superposition of x basis states. The spin state evolves according to Schrödinger's equation until a time (τ) later when a $\pi/2$ spin rotation pulse maps the coherence into an x basis probability amplitude. This is read out by a scattered photon during the next 4 ns pulse. The form of the signal, after dividing out by an exponential decay envelope, is

$$|\langle x+|R_{\sigma\mp}(\pi/2)U(\tau)\,\langle\sigma\pm|\Psi\rangle\rangle|^2 = \frac{1}{4}(1+\sin\Delta_e\tau), \tag{2}$$

where $R_{\sigma\mp} = \frac{1}{\sqrt{2}}(|x+\rangle\,\langle x+|\pm i\,|x+\rangle\,\langle x-|\pm i\,|x-\rangle\,\langle x+|+|x-\rangle\,\langle x-|)$, $U(\tau)$ is the time evolution operator, and Δ_e is the electron spin difference frequency.

Since, the radiative lifetime of the trion state ($\approx$ 1 ns) is longer than the spin precession period, the time τ varies randomly with an exponentially decaying probability. Upon measurement of the entangled photon, the spin state is re-initialized to $|z\pm\rangle$, serving as a measure of the phase of the generated spin coherence. One can view the timing resolution requirement ($\tau_r < 2\pi/\Delta_e$) as a quantum-eraser effect, where the photon detection must be sufficiently achromatic to avoid measuring the frequency mismatch between the two decay paths [21–26]. The data are shown in Fig. 4 along with fits of the first three periods to Eq. (2) using the experimentally determined spin difference frequency ($\Delta_e/2\pi = 7.35$ GHz).

From the fringe contrasts, we extract the conditional probabilities: $P(z-|\sigma+) = 0.70 \pm 0.05$, $P(z+|\sigma+) = 0.30 \pm 0.05$, $P(z-|\sigma-) = 0.31 \pm 0.04$, $P(z+|\sigma-) = 0.69 \pm 0.04$. We calculate a lower bound on the entanglement fidelity of $\mathcal{F} \geq 0.59 \pm 0.04$ using the expression $\mathcal{F} \geq 1/2(\rho_{Hx+,Hx+}+\rho_{Vx-,Vx-}-2\sqrt{\rho_{Hx-,Hx-}\rho_{Vx+,Vx+}}+\rho_{\sigma+z-,\sigma+z-}-\rho_{\sigma+z+,\sigma+z+}+\rho_{\sigma-z+,\sigma-z+}-\rho_{\sigma-z-,\sigma-z-})$ [20]. Here, we note that $2\pi/\Delta_e \approx 2.8 \times \tau_r$, so the reduction in fringe contrast is limited almost entirely by instrumental convolution. By convolving the theoretical signal with the detection system's instrument response function, and assuming a perfect correlation in the x basis, we estimate our experimentally realizable fidelity to be ≈ 0.7, putting the measured fidelity bound at 84% of the detector limited bound. The deviation from 100% of the maximum achievable fidelity is primarily from imperfect state initialization which is most pronounced in the V polarized (x basis) measurements. [32].

For quantum information applications such as QD spin-spin entanglement mediated by spin-photon entanglement, QD spin-photon entanglement is essential [18]. An important distinction of such a scheme is that the detector's timing resolution no longer plays a limiting role, allowing for higher magnetic fields, and therefore achievable fidelities approaching unity. The success rate of the x (z) basis measurement is approximately 0.06 s^{-1} (0.002 s^{-1}); however, the entanglement generation rate is given by the rate of entangled photons detected which is $DE \times 76$ MHz $= 3 \times 10^3$ s^{-1}. In a protocol similar to Moehring et al. [18], this would result in a spin-spin entanglement generation rate of approximately once per minute. Efficient spin readout should be possible by using a QD molecule sample capable of non-destructive spin measurement [34]. A feasibility analysis of using intermediate spin-photon entanglement to mediate distant QD spin-spin entanglement is given in the supplemental material [35]. Integrating these techniques has the potential to form a scalable QD spin architecture suitable for many quantum information applications.

After the submission of this work, two papers appeared in which results of a similar nature were reported [36, 37]. A discussion comparing the physics of these measurements to our result is given in the supplemental material [35].

Acknowledgements: This research is supported by NSF PHY0804114, PHY1104446; MURI W911NF-09-1-0406; AFOSR FA9550-09-1-0457; DARPA FA9550-10-1-0534; ARO W911NF-08-1-0487.

* dst@umich.edu

[1] D. Loss and D. P. DiVincenzo, Phys. Rev. A **57**, 120 (1998).

[2] A. Imamoğlu, D. D. Awschalom, G. Burkard, D. P. DiVincenzo, D. Loss, M. Sherwin, and A. Small, Phys. Rev. Lett. **83**, 4204 (1999).

[3] W. Yao, R.-B. Liu, and L. J. Sham, Phys. Rev. Lett. **95**, 030504 (2005).

[4] T. Ishikawa, S. Kohmoto, and K. Asakawa, Appl. Phys. Lett. **73**, 1712 (1998).

[5] P. Atkinson, S. Kiravittaya, M. Benyoucef, A. Rastelli, and O. G. Schmidt, Appl. Phys. Lett. **93**, 101908 (2008).

[6] A. Badolato, K. Hennessy, M. Atatüre, J. Dreiser, E. Hu, P. M. Petroff, and A. Imamoğlu, Science **308**, 1158 (2005).

[7] P. Gallo, M. Felici, B. Dwir, K. A. Atlasov, K. F. Karlsson, A. Rudra, A. Mohan, G. Biasiol, L. Sorba, and E. Kapon, Appl. Phys. Lett. **92**, 263101 (2008).

[8] M. Atatúre, J. Dreiser, A. Badolato, A. Högele, K. Karrai, and A. Imamoğlu, Science **312**, 551 (2006).

[9] X. Xu, Y. Wu, B. Sun, Q. Huang, J. Cheng, D. G. Steel, A. S. Bracker, D. Gammon, C. Emary, and L. J. Sham, Phys. Rev. Lett. **99**, 097401 (2007).

[10] D. Press, T. D. Ladd, B. Zhang, and Y. Yamamoto, Nature **456**, 218 (2008).

[11] E. D. Kim, K. Truex, X. Xu, B. Sun, D. G. Steel, A. S. Bracker, D. Gammon, and L. J. Sham, Phys. Rev. Lett. **104**, 167401 (2010).

[12] D. Kim, S. G. Carter, A. Greilich, A. S. Bracker, and D. Gammon, Nat. Phys. **7**, 223 (2011).

[13] C. Cabrillo, J. I. Cirac, P. García-Fernández, and P. Zoller, Phys. Rev. A **59**, 1025 (1999).

[14] L.-M. Duan, M. D. Lukin, J. I. Cirac, and P. Zoller, Nature **414**, 413 (2001).

[15] W. Yao, R.-B. Liu, and L. J. Sham, Phys. Rev. Lett. **95**, 030504 (2005).

[16] L.-M. Duan and C. Monroe, Rev. Mod. Phys. **82**, 1209 (2010).

[17] D. L. Moehring, M. J. Madsen, K. C. Younge, J. Kohn, P. Maunz, L.-M. Duan, C. Monroe, and B. B. Blinov, J. Opt. Soc. Am. B **24**, 300 (2007).

[18] D. L. Moehring, P. Maunz, S. Olmschenk, K. C. Younge, D. N. Matsukevich, L. Duan, and C. Monroe, Nature **449**, 68 (2007).

[19] Since submission of this paper, two papers have been published reporting entanglement be-

tween a QD spin and the photon polarization and a QD spin and the photon wavelength [36, 37].

[20] B. B. Blinov, D. L. Moehring, L.-M. Duan, and C. Monroe, Nature **428**, 153 (2004).

[21] J. Volz, M. Weber, D. Schlenk, W. Rosenfeld, J. Vrana, K. Saucke, C. Kurtsiefer, and H. Weinfurter, Phys. Rev. Lett. **96**, 030404 (2006).

[22] T. Wilk, S. C. Webster, A. Kuhn, and G. Rempe, Science **317**, 488 (2007).

[23] E. Togan, Y. Chu, A. S. Trifonov, L. Jiang, J. Maze, L. Childress, M. V. G. Dutt, A. S. Sorensen, P. R. Hemmer, A. S. Zibrov, and M. D. Lukin, Nature **466**, 730 (2010).

[24] J. R. Schaibley and P. R. Berman, J. Phys. B **45**, 124020 (2012).

[25] M. O. Scully and K. Drühl, Phys. Rev. A **25**, 2208 (1982).

[26] S. E. Economou, R.-B. Liu, L. J. Sham, and D. G. Steel, Phys. Rev. B **71**, 195327 (2005).

[27] J. R. Petta, A. C. Johnson, J. M. Taylor, E. A. Laird, A. Yacoby, M. D. Lukin, C. M. Marcus, M. P. Hanson, and A. C. Gossard, Science **309**, 2180 (2005).

[28] A. Greilich, D. R. Yakovlev, A. Shabaev, A. L. Efros, I. A. Yugova, R. Oulton, V. Stavarache, D. Reuter, A. Wieck, and M. Bayer, Science **313**, 341 (2006).

[29] D. Press, K. De Greve, P. L. McMahon, T. D. Ladd, B. Friess, C. Schneider, M. Kamp, S. Höfling, A. Forchel, and Y. Yamamoto, Nat. Phot. **4**, 367 (2010).

[30] J. G. Tischler, A. S. Bracker, D. Gammon, and D. Park, Phys. Rev. B **66**, 081310 (2002).

[31] R. H. Brown and R. Q. Twiss, Nature **177**, 27 (1956).

[32] Details of the correlation measurement analysis are given in the Supplementary Information.

[33] C. Piermarocchi, P. Chen, Y. S. Dale, and L. J. Sham, Phys. Rev. B **65**, 075307 (2002).

[34] D. Kim, S. E. Economou, S. C. Bădescu, M. Scheibner, A. S. Bracker, M. Bashkansky, T. L. Reinecke, and D. Gammon, Phys. Rev. Lett. **101**, 236804 (2008).

[35] See Supplementary Information.

[36] K. De Greve, L. Yu, P. L. McMahon, J. S. Pelc, C. M. Natarajan, N. Y. Kim, E. Abe, S. Maier, C. Schneider, M. Kamp, S. Höfling, R. H. Hadfield, A. Forchel, M. M. Fejer, and Y. Yamamoto, Nature **491**, 421 (2012).

[37] W. B. Gao, P. Fallahi, E. Togan, J. Miguel-Sanchez, and A. Imamoğlu, Nature **491**, 426 (2012).

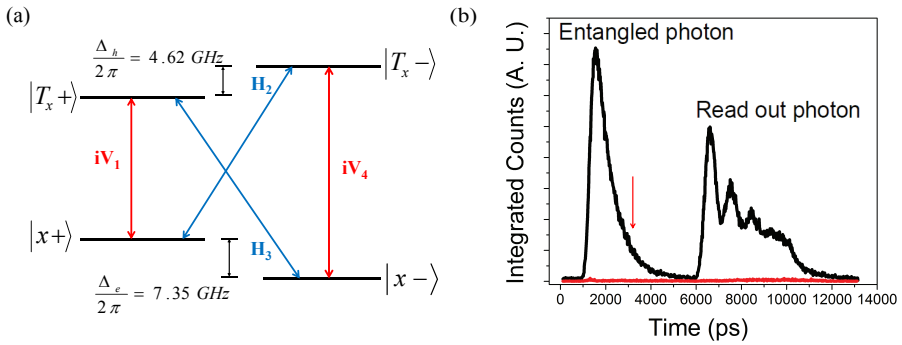

FIG. 1. (a) The effective four level system generated when a magnetic field is applied perpendicular to the QD growth axis. The selection rules are shown to be horizontal H (vertical (V)) where the i is included to illustrate the relative phase between the matrix elements. The subscripts label the transitions in order of increasing energy. The excited state (heavy hole) splitting ($\Delta_h/2\pi$), and the ground state (electron) splitting ($\Delta_e/2\pi$) are shown. (b) Time histogram of integrated fluorescence showing QD emission (black) from the excitation and readout/intialization pulses. The red shows the background level when the QD bias is tuned off resonance with the excitation lasers. The arrow indicates the temporal location of the rotation pulse used in the z basis measurements.

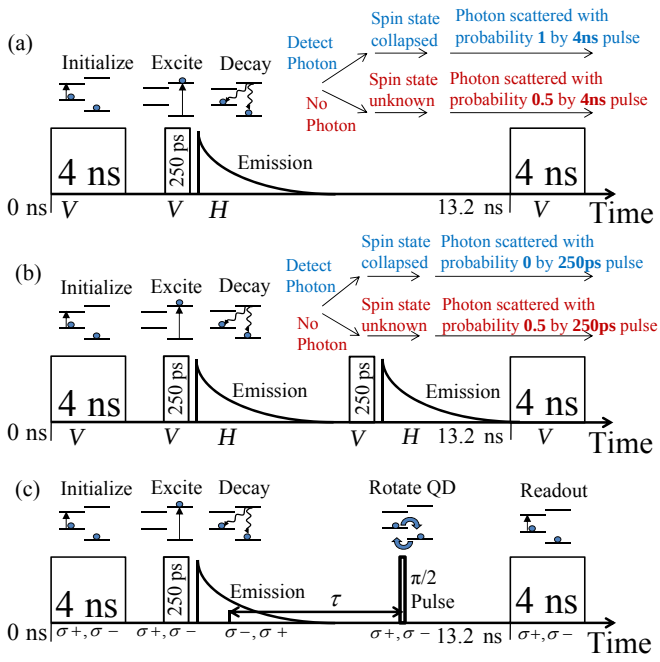

FIG. 2. (a) Pulse sequence used for $P(x+|H)$ measurement. After initialization, a 250 ps π pulse excites to $|T_x-\rangle$. Upon detection of a H polarized photon, the spin state ideally collapses to $|x+\rangle$ where the population is read out by the next 4 ns pulse. (b) To show anti-correlation ($P(x-|H)$) in an independent measurement, a second 250 ps π pulse is used to readout the remaining $|x-\rangle$ population after a H photon is detected. (c) To verify the entanglement, we perform the correlation measurement in the rotated (z) basis. Here, we excite with $\sigma\pm$ and detect $\sigma\mp$. A detuned $\pi/2$ Raman pulse is used after the 250 ps pulse to rotate the spin coherence into a probability amplitude that is read out by the following 4 ns pulse. The photon detection time is binned relative to the Raman pulse (τ) to observe the coincidence oscillations at the electron difference frequency.

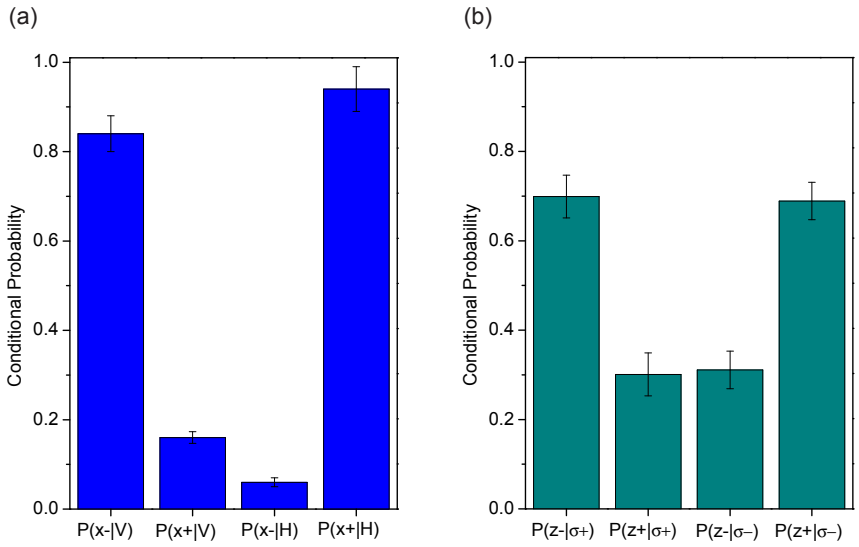

FIG. 3. Conditional probabilities showing the correlated nature of the entangled spin-photon state in two bases. (a) For the H,V measurements, corrected data are shown. (b) For the $\sigma\pm$ measurements, the conditional probabilities are extracted from fits shown in Fig. 4.

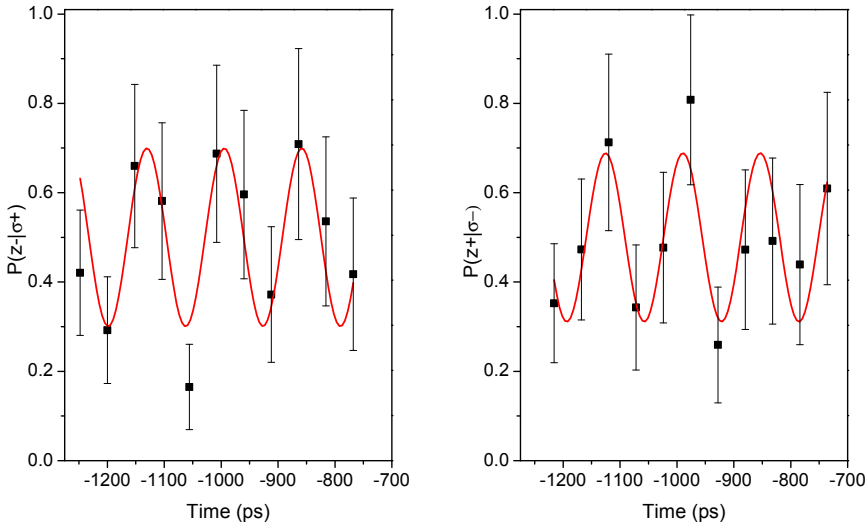

FIG. 4. Time resolved coincidence oscillations showing the QD spin coherence generated by projecting of the photon state onto $\sigma\pm$ for the left and right figures respectively. The time axis is taken relative to the QD spin rotation pulse which occurs at $t = 0$. The first three periods of the normalized data are fit to Eq. (2) using the experimentally determined difference frequency (7.35 GHz). The data show fringe contrasts of 0.40 ± 0.10 for $\sigma+$ and 0.38 ± 0.08 for $\sigma-$. Note that because we remove the exponential envelope by division, the relative noise increases with time.